Traveling-Wave Fault Locating for Multiterminal and Hybrid Transmission Lines

Stephen Marx
Bonneville Power Administration

Yajian Tong and Mangapathirao V. Mynam
Schweitzer Engineering Laboratories, Inc.

Traveling-Wave Fault Locating for Multiterminal and Hybrid Transmission Lines

Stephen Marx, *Bonneville Power Administration*

Yajian Tong and Mangapathirao V. Mynam, *Schweitzer Engineering Laboratories, Inc.*

Abstract—**Multiterminal lines are originally constructed or expanded from two-terminal lines for economic reasons. Hybrid lines with both overhead conductor and underground cable sections are constructed to cross difficult terrain without the cost of constructing the entire line as a cable line. With these transmission lines gaining popularity, specifically at subtransmission voltage levels, there is a need for accurate fault-locating methods for these lines. Traveling-wave fault locating (TWFL) methods provide fault location with a typical accuracy on the order of one tower span. This paper discusses how the two-terminal TWFL method can be extended to multiterminal and hybrid lines, including multiterminal lines with a combination of overhead conductor and underground cable sections. Laboratory tests and field events are included to explain and illustrate the performance of the discussed fault-locating methods on these lines. The paper also discusses how to measure traveling-wave line propagation time, which is needed to set the fault locator for the best possible accuracy.**

I. INTRODUCTION

Accurate and instantaneous fault locating is an extremely valuable function for power utilities. Accurate fault locating shortens patrol times, reduces potential recurring faults, and aids system reconfiguration following a permanent fault. Instantaneous access to accurate fault location allows for control applications, such as autoreclose cancel, to be used on hybrid lines [1]. Traveling-wave fault locators provide accurate fault location on the order of one to two tower spans. Traditionally, this technology was only available in standalone traveling-wave fault locators, which is one of the reasons why it was only applied on extra-high-voltage lines. Utilities were not able to justify the application of the traveling-wave fault locators for low voltage levels. As line relays are now available with this functionality, many utilities have embraced this approach and applied this technology to locate faults on transmission systems.

For economic reasons, two-terminal lines are sometimes extended to multiterminal lines. These multiterminal lines are gaining more popularity for integrating renewable resources or serving remote loads. Using hybrid lines with both overhead conductor and underground cable sections is a viable approach when constructing lines that cross difficult terrain. Locating faults on these lines is just as critical as locating faults on two-terminal lines.

This paper presents how two-terminal traveling-wave fault locating (TWFL) methods can be applied to multiterminal and hybrid lines. Laboratory test results are provided to demonstrate the proposed fault-locating method for multiterminal lines.

Traveling-wave line propagation time is a key parameter for accurate fault locating. We illustrate a recommended practice to measure the traveling-wave line propagation times on multiterminal and hybrid lines.

Finally, we discuss how Bonneville Power Administration (BPA) applied traveling-wave fault locators embedded in line relays to locate faults on a three-terminal line. We show the performance of the fault-locating method for faults on their Swan Valley-Teton-Drummond 115 kV line. We discuss a permanent fault on this line, the procedure the crew followed to reconfigure the line, and how the fault location aided the crew in this reconfiguration process.

II. TWFL FOR TWO-TERMINAL TRANSMISSION LINES

A. Two-Terminal Homogeneous Lines

Traveling waves are launched when a fault occurs on a transmission line, and they propagate toward the terminals. Relays equipped with traveling-wave functions measure these high-frequency signals. For two-terminal homogeneous lines where traveling-wave propagation velocity is constant, a traveling-wave fault locator uses the arrival time of the first traveling wave captured by synchronized devices at both terminals, the line length, and the traveling-wave propagation time to calculate the fault location [2]. Fig. 1 depicts a two-terminal homogeneous line and the fault location M from Terminal S, which can be calculated as shown in (1).

$$M = \frac{L}{2} \cdot \left(1 + \frac{t_S - t_R}{T}\right) \qquad (1)$$

where:

t_S is when the first traveling wave arrives at Terminal S.

t_R is when the first traveling wave arrives at Terminal R.

L is the line length.

T is the traveling-wave propagation time.
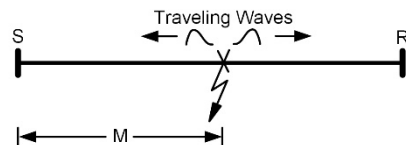
Fig. 1.   Traveling waves on a two-terminal homogeneous line

Fig. 2 shows the traveling waves recorded for an example fault on a 230 kV, 28.4 km (17.65 mi) line. The time difference between the first traveling-wave arrival times ($t_S - t_R$) for this C-Phase-to-ground (CG) fault is 18.220 μs and the traveling-

wave propagation time is 99.88 µs. Using (1), we can calculate the fault location to be 16.79 km (10.43 mi).
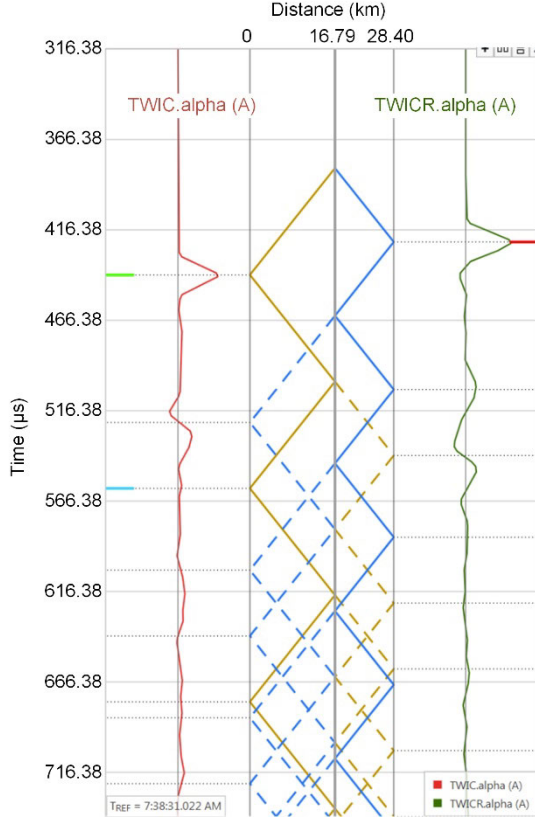
Fig. 2.   Measured alpha current traveling waves [2] for a CG fault

B.   Two-Terminal Hybrid Lines

When a transmission line consists of overhead conductors and underground cables, the traveling-wave propagation velocity is different in each section. The traveling-wave propagation velocity of an underground cable is slower than that of overhead conductors, typically by a factor of about 2. This difference in the traveling-wave propagation velocity makes it challenging to calculate fault location using (1).

Fig. 3 shows an example two-terminal, three-section line where Sections SD and ER are overhead conductors and Section DE is an underground cable.
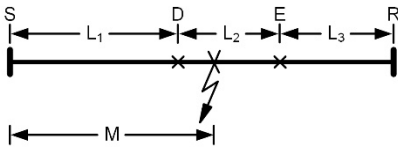
Fig. 3.   Example of a two-terminal, three-section transmission line

Reference [1] summarizes the approach for locating faults on hybrid lines as follows:

1.   Calculate the fault location (M^*) with (1) as if the line were homogeneous.
2.   Calculate the propagation time (t^*) corresponding to the fault location (M^*) assuming the line is homogeneous.
3.   Calculate the actual fault location (M) corresponding to the propagation time (t^*) using the distance and propagation time characteristics of the actual (nonhomogeneous) line.

Fig. 4 illustrates this process. T_1 is the traveling-wave propagation time of L_1. T_2 is the traveling-wave propagation time of L_2. T_3 is the traveling-wave propagation time of L_3.
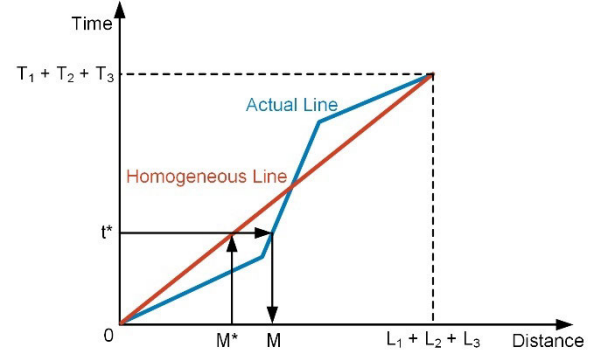
Fig. 4.   Illustration of the three-step method to locate a fault on a two-terminal hybrid line

Alternatively, because of the piecewise linear relationship between the fault location and the traveling-wave time difference between two terminals, we can directly calculate the fault location M from Terminal S using the traveling-wave time difference $\Delta t = t_S - t_R$, as shown in (2).

$$M = \begin{cases} \dfrac{L_1}{2T_1}\left(\Delta t + T_1 + T_2 + T_3\right), \Delta t_S \le \Delta t \le \Delta t_D \\[2mm] L_1 + \dfrac{L_2}{2T_2}\left(\Delta t - T_1 + T_2 + T_3\right), \Delta t_D \le \Delta t \le \Delta t_E \\[2mm] L_1 + L_2 + \dfrac{L_3}{2T_3}\left(\Delta t - T_1 - T_2 + T_3\right), \Delta t_E \le \Delta t \le \Delta t_R \end{cases} \quad (2)$$

where:

Δt_S is $-T_1 - T_2 - T_3$.

Δt_D is $T_1 - T_2 - T_3$.

Δt_E is $T_1 + T_2 - T_3$.

Δt_R is $T_1 + T_2 + T_3$.

III. TWFL FOR MULTITERMINAL TRANSMISSION LINES

A. TWFL Principles for Three-Terminal Lines

Locating faults on a multiterminal line can be done in two ways. Either the faulted section is identified first and the multiterminal line is reduced to an effective two-terminal line to estimate the fault location [3], or traveling-wave fault locations are calculated multiple times on different two-terminal sections to find the true fault location. Both approaches require the traveling-wave fault locator at each terminal to be synchronized or to have a high-quality clock and require line information such as the length and the traveling-wave propagation time of every section.

Fig. 5 shows an example three-terminal line. For a fault on the section between Terminal N and Tap D, traveling waves are launched and propagate toward Terminal N and Tap D. At Tap D, the traveling wave splits and propagates toward Terminals S and R. If we calculate the fault location between Terminals S and N using the two-terminal method mentioned in Section II, we can find the actual fault location. However, if we calculate the fault location between Terminals S and R, we will find the location to be at the tap. Therefore, calculating fault locations between every two terminals is helpful to clarify the actual fault location.
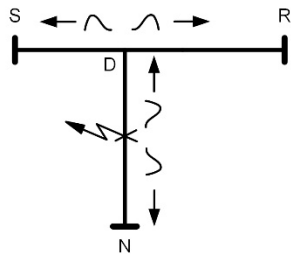
Fig. 5.   Three-terminal line with a fault between Terminal N and Tap D

The following three-step fault-locating process can be executed to find the true fault position:

1. Conduct a two-terminal TWFL calculation between every two terminals (see the examples in Fig. 6, Fig. 7, and Fig. 8—dashed fault symbols indicate the calculated fault location, while solid fault symbols indicate the actual fault location).
2. Identify the terminal from which all the calculated fault locations match within a specified tolerance (e.g., 0.1 mi).
3. Average the results from Step 2 if they are within the specified tolerance. The true fault location is this averaged value.
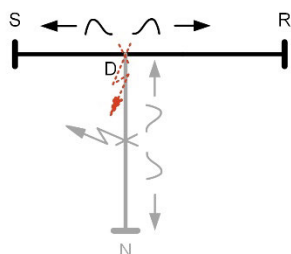
Fig. 6.   TWFL calculation between Terminals S and R
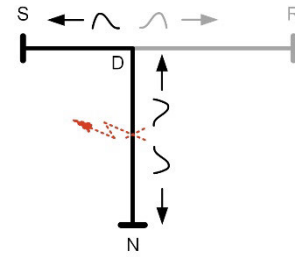
Fig. 7.   TWFL calculation between Terminals S and N
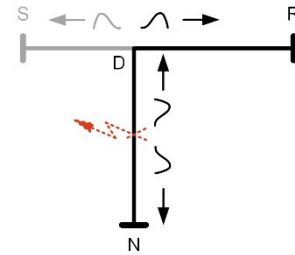
Fig. 8.   TWFL calculation between Terminals R and N

A homogenous line with the configuration from Fig. 5 was modeled in an Electromagnetic Transients Program (EMTP); the line parameters used are specified in Table I. The simulation result was converted and uploaded into the relay for playback [4]. The line operated at 138 kV, and a CG fault occurred 20 mi from Terminal N on Section ND. Fig. 9, Fig. 10, and Fig. 11 show the voltages and currents at Terminals S, R, and N, respectively. Fig. 12 shows the alpha current traveling waves of the faulted phase.

TABLE I
THREE-TERMINAL LINE DATA USED IN THE EMTP STUDY

Section	Length (mi)	Traveling-Wave Propagation Time (μs)
SD	8	43
RD	23	123.625
ND	27	145.125
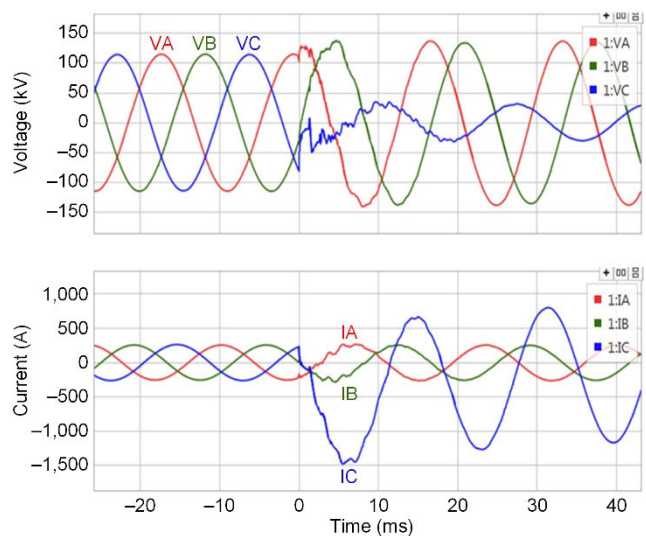
Fig. 9.   Voltages and currents at Terminal S
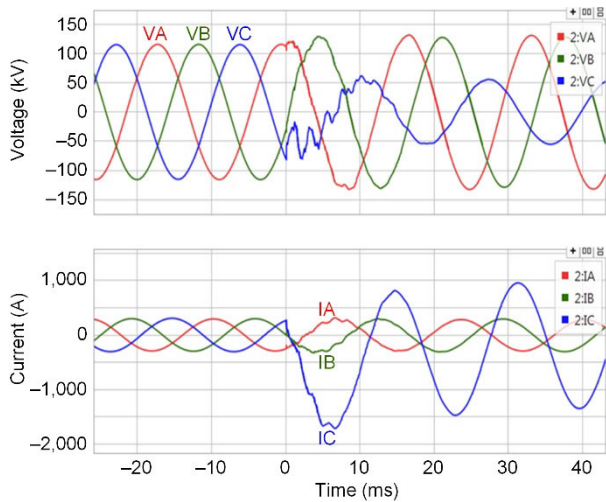
Fig. 10. Voltages and currents at Terminal R
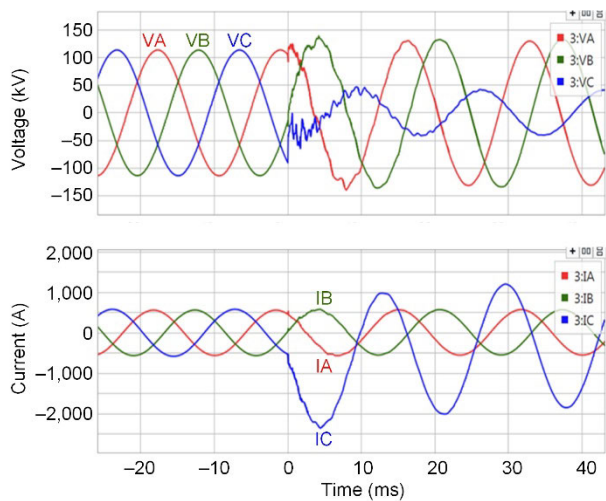
Fig. 11. Voltages and currents at Terminal N
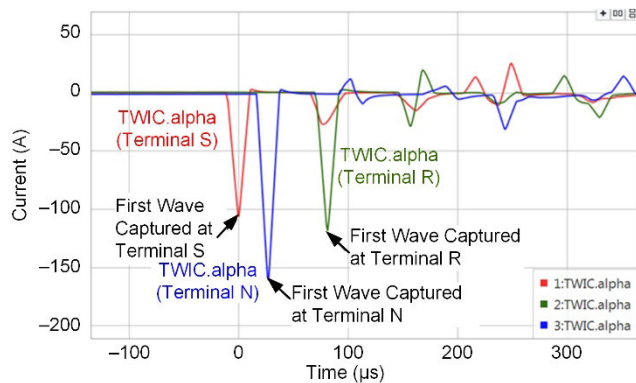
Fig. 12. Alpha current traveling waves of Phase C at each terminal for the simulated system from Fig. 5

The traveling-wave arrival times past the top of a second at Terminals S, R, and N are as follows:

$t_S = 0.217091736$ s

$t_R = 0.217172921$ s

$t_N = 0.217118717$ s

Since the line is homogenous, (1) can be used to calculate the fault location on the section between Terminals S and R.

Otherwise, (2) would be used to account for hybrid sections. The fault location calculated from Terminal S is shown in (3).

$$M_1 = \frac{8+23}{2} \bullet \left(1 + \frac{217091.736 - 217172.921}{43 + 123.625}\right) = 7.948 \text{ mi} \quad (3)$$

The fault location could also be calculated as 23.052 mi from Terminal R.

Similarly, with (1) used for Section SN, the fault location calculated from Terminal S is as shown in (4).

$$M_2 = \frac{8+27}{2} \bullet \left(1 + \frac{217091.736 - 217118.717}{43 + 145.125}\right) = 14.990 \text{ mi} \quad (4)$$

The fault location could also be calculated as 20.010 mi from Terminal N.

Again, if the calculation is performed on Section RN, the fault location calculated from Terminal R is as shown in (5).

$$M_3 = \frac{23+27}{2} \bullet \left(1 + \frac{217172.921 - 217118.717}{123.625 + 145.125}\right) = 30.042 \text{ mi} \quad (5)$$

The fault location could also be calculated as 19.958 mi from Terminal N.

Table II summarizes the calculated fault locations (which are expressed as the distance from the column terminals) between every two terminals. The calculation from Terminal N gives the fault location results of 20.010 mi and 19.958 mi, which are within 0.1 mi of each other. Averaging these two values indicates that the fault location is 19.984 mi from Terminal N. Using an averaged fault location helps lower the impact of traveling-wave dispersion, noise, time-stamping accuracy, and so on.

TABLE II
FAULT LOCATIONS CALCULATED ON EACH TWO-TERMINAL SECTION

Terminal	S	R	N
S	–	7.948 mi	14.990 mi
R	23.052 mi	–	30.042 mi
N	20.010 mi	19.958 mi	–

It is worth noting that in the three-step procedure to find the true fault location, all the fault locations calculated from one terminal should match each other within a predefined tolerance. However, it is possible that no terminal will exist from which all the calculated fault locations match. There could be several reasons for this; the clock(s) in one or more terminals may not be strictly synchronized, the measurement of the traveling-wave propagation time may not be accurate, and so on. These factors could result in a calculated fault location that is different from the actual fault location.

For example, if the clock used at one terminal is faster than the reference time, the calculated fault location will be farther away from the terminal than it should be. Also, when a larger traveling-wave propagation time than the actual propagation time is used, the calculated fault location moves toward the middle point of the section where the traveling-wave propagation time is inaccurately set. Although detailed discussion is not included here, as it is beyond the scope of this

paper, the calculated results should match within a tolerance for accurate fault-location reporting.

B. Generalization of TWFL for Lines With Arbitrary Numbers of Terminals

The three-step analysis process outlined in Section III can be applied to multiterminal hybrid lines such as the one shown in Fig. 13. It is worth noting that it does not matter whether the lines connecting any two terminals are homogenous or hybrid; we do not differentiate between the two, because two-terminal TWFL methods are available to both homogeneous and hybrid lines.
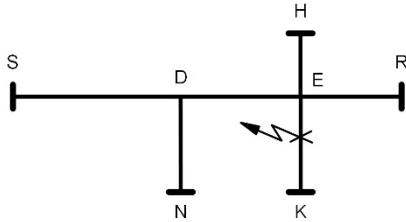
Fig. 13. Example of a multiterminal line

Fig. 14, Fig. 15, Fig. 16, and Fig. 17 (dashed fault symbols indicate the calculated fault location, while solid fault symbols indicate the actual fault location) illustrate the fault location calculations between Terminal S and the rest of the terminals. The same process can then be applied to the other terminals.
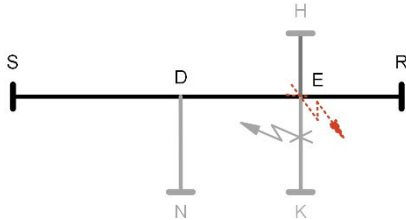
Fig. 14. TWFL calculation between Terminals S and R
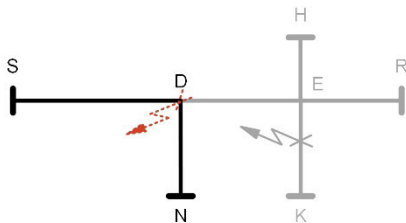
Fig. 15. TWFL calculation between Terminals S and N
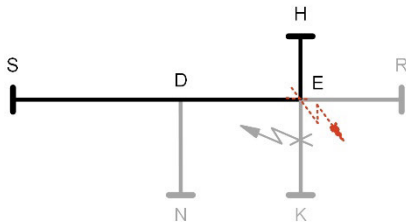
Fig. 16. TWFL calculation between Terminals S and H
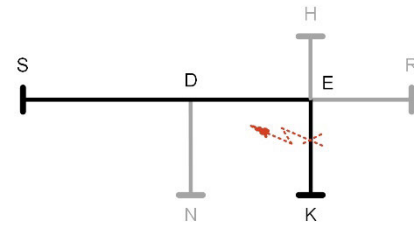
Fig. 17. TWFL calculation between Terminals S and K

For simplicity and convenience, a homogenous line of the same topology shown in Fig. 13 was modeled in an EMTP. The line data are specified in Table III. A B-Phase-to-ground (BG) fault was simulated 12 mi from Terminal K, and the result was played back through the relays.

TABLE III
FIVE-TERMINAL LINE DATA USED IN THE EMTP STUDY

Section	Length (mi)	Traveling-Wave Propagation Time (µs)
SD	18	96.75
ND	8	43
RE	23	123.625
HE	11	59.125
KE	17	91.375
DE	7	37.625

Fig. 18 shows the alpha current traveling waves of Phase B at all the terminals. Their associated traveling-wave arrival times are as follows:

t_S = 0.205173011 s
t_R = 0.205162188 s
t_N = 0.205118846 s
t_H = 0.205097230 s
t_K = 0.205075668 s
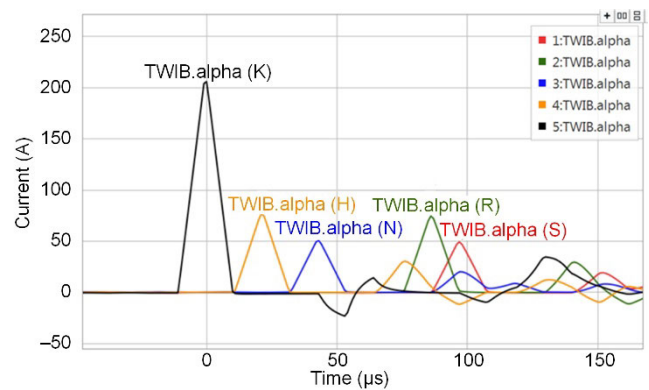
Fig. 18. Alpha current traveling waves at each terminal for a BG fault on the five-terminal line modeled in the EMTP study

Using these time stamps, we can calculate the fault location on each two-terminal section, as shown in Table IV. Fault locations calculated between Terminal K and the rest generate the "same result" (i.e., the calculations are within a 0.1 mi tolerance of each other). Thus, the fault will be (11.945 + 11.952 + 11.983 + 11.994) / 4 = 11.968 mi from Terminal K.

TABLE IV
FAULT LOCATIONS CALCULATED ON EACH TWO-TERMINAL SECTION

Terminal	S	R	N	H	K
S	–	25.007 mi	18.039 mi	25.049 mi	30.055 mi
R	22.993 mi	–	23.032 mi	23.043 mi	28.048 mi
N	7.961 mi	12.993 mi	–	15.011 mi	20.017 mi
H	10.951 mi	10.957 mi	10.989 mi	–	16.006 mi
K	11.945 mi	11.952 mi	11.983 mi	11.994 mi	–

IV. MEASURING TRAVELING-WAVE LINE PROPAGATION TIME

Line constant programs, which provide propagation times based on tower structure and conductor properties, are available in most EMTPs. To achieve higher accuracy with the TWFL method, we recommend measuring traveling-wave propagation time from fault events and line energization [1].

When the example two-terminal, three-section line in Fig. 3 is energized from one terminal, a traveling wave is launched and propagates toward the other terminal. Because of the change in the line's characteristic impedance at each transition point, part of the traveling wave is reflected toward the sending terminal and part of it propagates forward. The traveling-wave propagation time of each section can be measured with the help of an estimated traveling-wave propagation time based on the line length and the estimated traveling-wave velocity of each section.

The Bewley lattice diagram [5] shown in Fig. 19 illustrates how traveling waves propagate and reflect in a system.
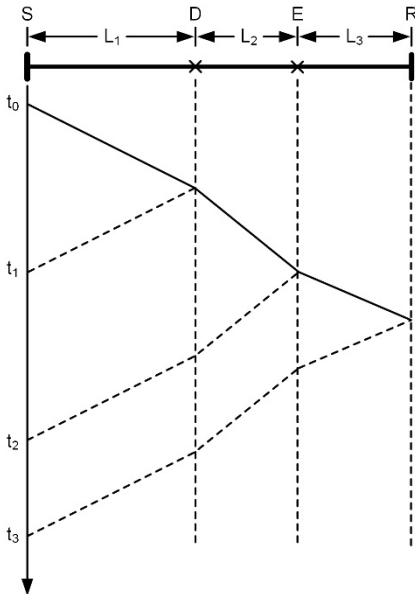
Fig. 19. Bewley diagram of hybrid line energization

Consider t_0 to be the time of the line energization from Terminal S. Using each section's estimated traveling-wave

propagation time, we can narrow down the time frame to identify reflected traveling waves from each discontinuity. From Fig. 19, a traveling wave arriving at t_1 is the reflection from the first transition point D; thus, the traveling-wave propagation time of Section SD is $(t_1 - t_0) / 2$. Similarly, the traveling-wave propagation time of Sections DE and ER are $(t_2 - t_1) / 2$ and $(t_3 - t_2) / 2$, respectively.

For hybrid lines specifically, it is beneficial to use energization events from both terminals to identify reflections from transitions close to each terminal [1]. Fig. 20 shows a one-line diagram of an example 138 kV line consisting of one overhead conductor section (SD) and one underground cable section (DR). We used energization events from both terminals to identify the traveling-wave propagation time for Sections SD and DR.
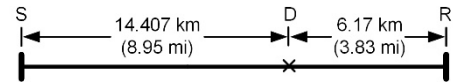
Fig. 20. One-line diagram showing the overhead conductor and underground cable sections

Fig. 21 shows the energized phase (Phase C) current and its associated alpha current traveling wave from Terminal S. Assuming that the traveling-wave propagation velocity of the overhead conductor is 98 percent of the speed of light, the estimated traveling-wave propagation time of the overhead conductor is 49 µs. Thus, the reflection from the transition point should be two times 49 µs, or 98 µs. With this information, we can determine that the reflected traveling wave from the transition point is 97 µs after the first traveling wave.
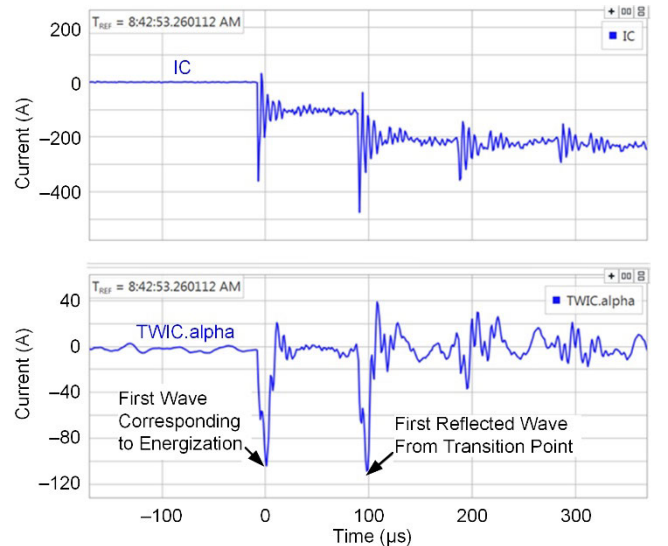
Fig. 21. Line energization event report from Terminal S

Similarly, Fig. 22 shows the energized phase (Phase B) current and its associated alpha current traveling wave from Terminal R. Assuming the traveling-wave propagation velocity of the underground cable is 55 percent of the speed of light, the reflected traveling wave from the transition point can be found at 74 µs after the first traveling wave.

Therefore, the measured traveling-wave propagation times are 48.5 µs (97 µs / 2) and 37 µs (74 µs / 2) for Sections SD and

DR, respectively. For multiterminal lines, we can use a similar approach to measure the traveling-wave propagation time.
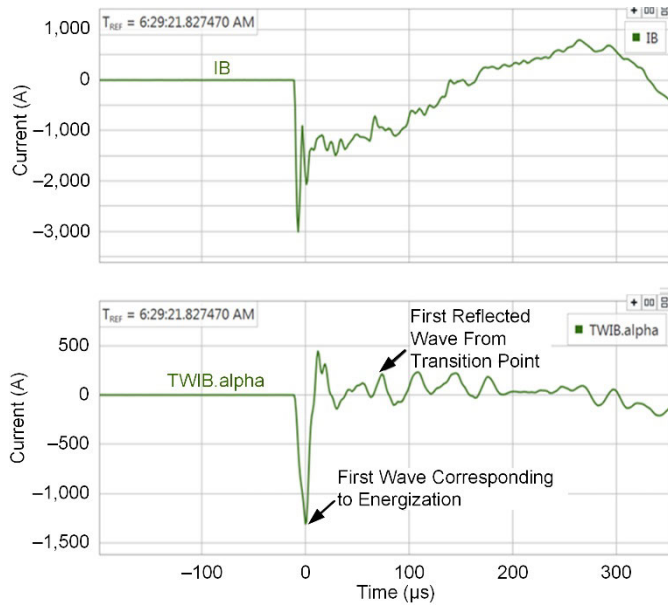
Fig. 22. Line energization event report from Terminal R

V. PERFORMANCE OF THE TRAVELING-WAVE FAULT LOCATOR ON A THREE-TERMINAL, 115 KV LINE

Fig. 23 shows a three-terminal, 115 kV line between the Swan Valley, Teton, and Drummond substations that BPA owns and operates. Two lines share the right-of-way between the Swan Valley and Teton terminals. Line 2 does not include taps. Line 1 has a tap (T_1) midway between the Swan Valley and Teton terminals that goes to the Targhee substation and connects to the Drummond terminal. There is only one circuit breaker at Targhee with no main auxiliary bus configuration. The line between Tap T_1 and Targhee is tapped twice; Tap T_2 goes to the Victor substation with two 115:46 kV transformers and Tap T_3 (inside the Targhee substation) connects to a 115:46 kV transformer and a 115:12.5 kV transformer.

Identifying the faulted sections and locating faults on Swan Valley-Teton-Drummond Line 1 is challenging. The area between Taps T_1 and T_3 is flat farmland mixed with residential communities. There is also a marshy area, making it difficult to access the power line. The line section from Swan Valley to Tap T_1 goes across Pine Creek Pass with an elevation of over 6,200 ft. The line section from Teton to Tap T_1 goes across Teton Pass with an elevation of over 8,500 ft. Because of the area and terrain, the power lines are subjected to faults caused by wind, ice unloading resulting in galloping, lightning, bird excrement contamination, and insulators being shot with firearms. Most faults are caused by bird contamination and ice.

When a fault occurs on this three-terminal line (Swan Valley-Teton-Drummond Line 1), the taps at Victor and Targhee make it so that two towns and a ski resort are blacked out. For a temporary fault, the outage lasts as long as the reclose time is set for, typically on the order of 1 second. A permanent fault creates a loss of power to everyone who does not have a backup generator.
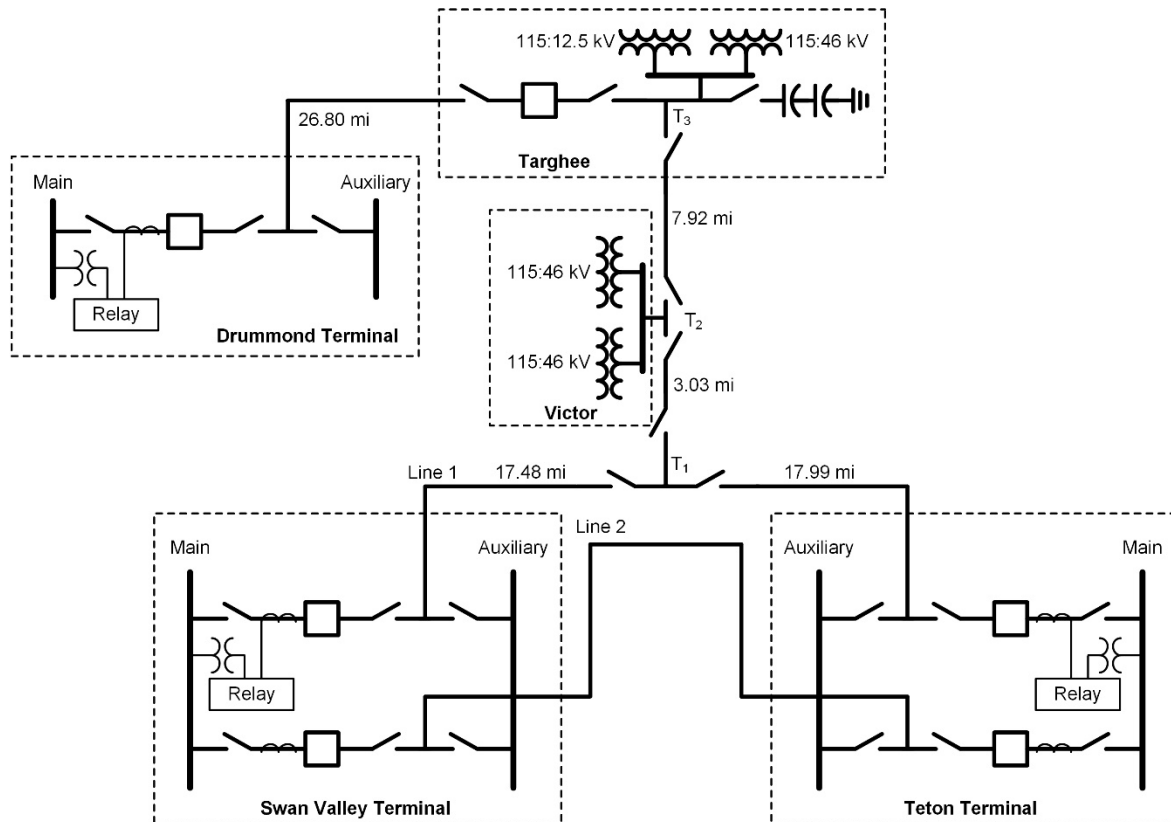
Fig. 23. BPA one-line diagram showing the Swan Valley-Teton-Drummond system

Swan Valley-Teton Line 1 is made up of 18 different sections. Six of the sections are double-circuit configurations with Swan Valley-Teton Line 2. Twelve of the sections are single-circuit configurations. Eight of the circuits use lattice steel, five use wood poles, and five use steel poles. On the double-circuit sections, the conductors are either in vertical or delta configurations. On the single-circuit sections, the conductors are configured either horizontally or vertically. The zero-sequence mutual coupling along with multiple sections and different tower configurations pose a challenge to impedance-based fault-locating methods.

A. Fault Locator Experience

BPA's previous installations of line relays with TWFL functionality on two-terminal lines successfully demonstrated the exceptional accuracy of the applied traveling-wave fault locator [2]. It provided accuracy of one to two tower spans. With this success on finding faults on two-terminal lines, BPA decided to evaluate the traveling-wave fault locator on Swan Valley-Teton-Drummond Line 1.

Line relays with TWFL functionality were installed at the Swan Valley, Teton, and Drummond substations. A 64 kbps communications channel exists between the Swan Valley and Drummond substations. Relays at these two substations are configured to locate faults on the two-terminal line between the Swan Valley and Drummond terminals. For faults in the section between Teton and Tap T_1, relays at the Swan Valley and Drummond substations report the fault location at Tap T_1. Therefore, BPA designed a tool based on the method discussed in Section III to calculate the overall fault location on this three-terminal line. The user provides the first traveling-wave arrival time at each terminal, the line length, and the propagation time of each section. Relays provide the traveling-wave arrival times in event records and via communications protocols such as DNP3. BPA uses the traveling-wave arrival times included in the event reports. Fig. 24 shows the spreadsheet tool BPA used to calculate the fault location.

Fault Times		
Swan Valley	**Teton**	**Drummond**
37.011171906 sec	37.011175528 sec	37.011050105 sec

LL from Drummond to Targhee	26.80	miles
LL from Swan Valley to Tap	17.48	miles
LL from Targhee to Tap	10.95	miles
LL from Teton to Tap	17.99	miles
LL from Swan Valley to Teton	35.47	miles
LL from Drummond to Swan Valley	55.23	miles
LL from Drummond to Teton	55.74	miles
Line Propagation Coefficient	0.98820	per unit
Speed of Light (miles/sec)	186282.39705	mi/sec
Distance from Swan Valley to Teton	17.4016	miles
Distance from Swan Valley to Drummond	38.8258	miles
Distance from Teton to Swan Valley	18.0684	miles
Distance from Teton to Drummond	39.4142	miles
Distance from Drummond to Swan Valley	16.4042	miles
Distance from Drummond to Teton	16.3258	miles

Fig. 24. Spreadsheet used by BPA for offline calculation of fault location from three terminals

During the BPA evaluation, a CG fault occurred on Swan Valley-Teton-Drummond Line 1. Fig. 25 shows the phase currents captured at Swan Valley, Teton, and Drummond, respectively. Fig. 26 shows the alpha current traveling waves of the faulted phase at all three terminals. The recorded traveling wave arrival times for the faulted phase alpha currents in the format of hh:mm:ss.ns are as follows:

Swan Valley—21:21:37.011171906
Teton—21:21:37.011175528
Drummond—21:21:37.011050105
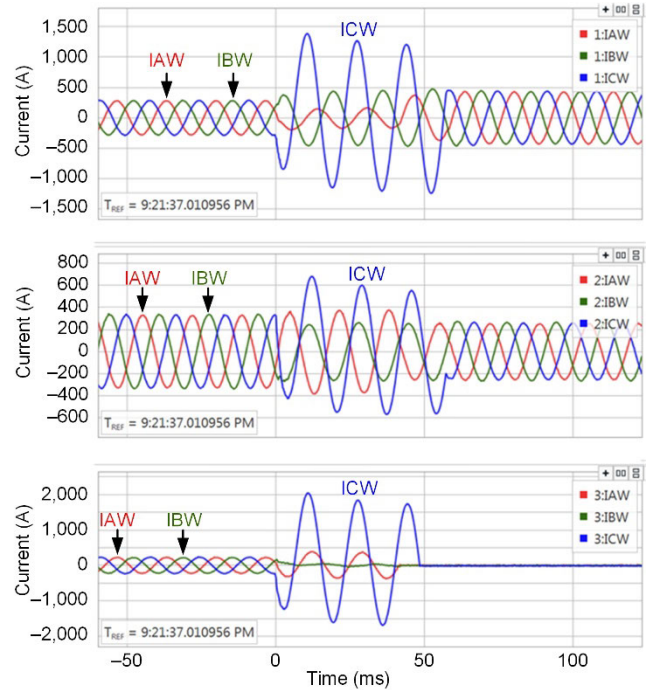
Fig. 25. Phase currents of Swan Valley (top), Teton (middle), and Drummond (bottom) for a CG fault 16.395 mi from Drummond
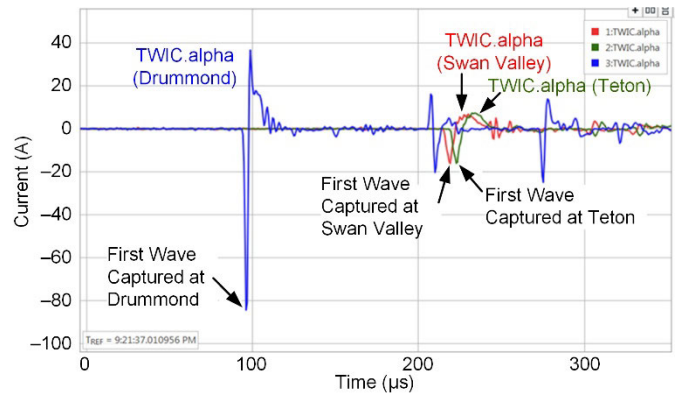
Fig. 26. Alpha current traveling waves at Swan Valley, Teton, and Drummond for a CG fault 16.395 mi from Drummond

As shown in Fig. 24, BPA estimated the fault location for this event as 16.365 mi ((16.4042 mi + 16.3258 mi) / 2) from Drummond. The line crew found an insulator that was contaminated by a bird (see Fig. 27) 16.395 mi from Drummond on the Drummond-Targhee section. Note in Fig. 24 that BPA used the traveling-wave propagation velocity (the line propagation coefficient times the speed of light) instead of the

traveling-wave propagation time to calculate the fault location. The traveling-wave propagation time could be alternatively obtained by dividing the line length by the traveling-wave propagation velocity. However, we recommend using traveling-wave propagation time if it can be measured for better accuracy.

It should also be mentioned that, as shown in Fig. 25, the currents at Swan Valley and Teton were found still flowing after the fault was cleared, while the currents at Drummond went to zero. This is because the fault was cleared by circuit breakers at Drummond and Targhee, which also verifies that the calculated fault location was in the correct zone. On this three-terminal line, there are multiple protection zones but only one fault location zone (Swan Valley-Teton-Drummond Line 1) based on the TWFL method.

Table V shows more field events on Swan Valley-Teton-Drummond Line 1.

Fig. 27.   Bird-contaminated insulator 16.395 mi from Drummond

B.   Fault Location Aids System Reconfiguration

In the past, for a permanent fault, a line crew would drive along the power line until they found the fault. At times, they would guess on which section the fault might be. This approach caused long outage times and sometimes caused additional disturbances on the network when reclosing on the faulted section if a guessed location was wrong. However, with the TWFL method, the fault location can be identified more accurately.

Recently, a permanent A-Phase-to-B-Phase (AB) fault occurred on Swan Valley-Teton Line 1. Ice unloading followed by galloping was assumed to be the cause of the fault. The circuit breakers at Teton, Swan Valley, and Targhee tripped to clear the fault. BPA was notified by local operators that the line was locked out after reclose. Initially, the fault was assumed to be between the Targhee substation and the Tap T_1 section of the line because there had been multiple faults on this section of the line in the past. The operators proceeded to isolate the line from Targhee to Tap T_1 so that the Swan Valley-Teton section could be closed in.

Based on the recorded traveling waves from the relay (see Fig. 28), BPA analyzed the traveling-wave arrival times between Swan Valley and Drummond. The calculated location was 37.690 mi from Drummond. Thus, the fault could have been at Tap T_1. Then, another two-terminal traveling-wave fault location was calculated between Teton and Swan Valley. BPA obtained a location of 7.069 mi from Teton. This result put the fault between Teton and Tap T_1. After opening the line disconnects at Tap T_1, the operators closed the circuit breaker at Teton. The line was faulted, and a second traveling-wave measurement was captured, as shown in Fig. 29. This time, BPA used the single-end TWFL method described in [6] to calculate the distance to the fault as 7.163 mi from the Teton terminal. Based on these two calculations, it appeared that the fault was between Tap T_1 and Teton.

TABLE V
FAULT LOCATION FOR FAULTS ON SWAN VALLEY-TETON-DRUMMOND LINE 1

Event Date	Fault Type	Fault Reason	Actual Fault Location From Drummond (mi)	Calculated Fault Location From Drummond (mi)	Error (ft)
January 5, 2015	BG	Transformer bushing failure	26.79	26.74	−264
April 1, 2015	CG	Flashed insulator	27.95	27.91	−211
May 5, 2015	AG	Flashed insulator	27.74	27.66	−422
October 29, 2015	AG	Bird contamination	36.47	36.44	−158
August 18, 2018	BG	Fire	17.37	17.57	1056
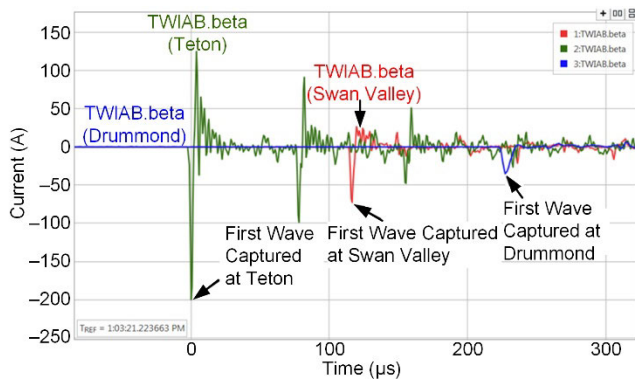
Fig. 28. Beta current traveling waves [2] at Swan Valley, Teton, and Drummond for an AB fault
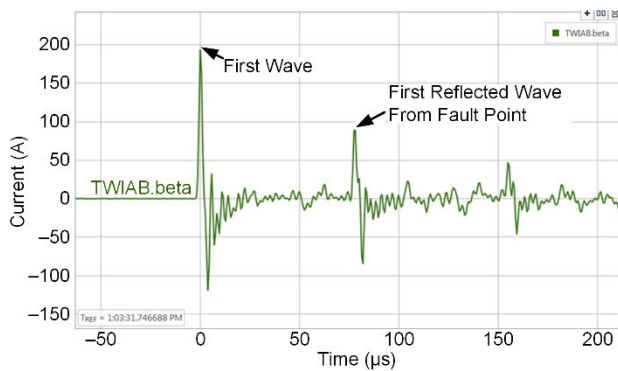
Fig. 29. Beta current traveling wave at Teton for a close onto an AB fault

The section of line between Tap T_1 and Teton is on the eastern slope of Teton Pass going into Jackson Hole, Wyoming. The predicted fault distance was mid-span between two towers (see Fig. 30). Because of the canyon slope and rough terrain, BPA was unable to get close enough to positively identify where the fault was. They patrolled the line with helicopters, but with the winds coming up the canyon slope, it was difficult to get close enough to the line to identify the fault. A similar fault occurred in the same location four months earlier, and BPA was not able to identify that fault either. However, BPA has assumed that these faults were caused by ice unloading, and they are working to change the line configuration in this area to eliminate future recurring faults.

Fig. 30. Faulted line section between Teton and Tap T1 for an AB fault

Overall, having accurate fault location on these complex system topologies will help in intelligently reconfiguring the system, rather than relying on guesswork.

VI. CONCLUSION

Accurate fault location on multiterminal and hybrid lines is critical. This paper presents TWFL methods for these types of lines. The described methods are verified using EMTP studies and field events. The calculated fault locations for these events are within one to two tower spans of the actual locations. The paper also provides methods to measure the traveling-wave line propagation times on these lines. Line relays embedded with TWFL functionality are available to help users accurately locate faults on transmission lines.

VII. REFERENCES

[1] B. Kasztenny, A. Guzmán, M. V. Mynam, and T. Joshi, "Locating Faults Before the Breaker Opens – Adaptive Autoreclosing Based on the Location of the Fault," proceedings of the 71st Annual Conference for Protective Relay Engineers, College Station, TX, March 2018.

[2] E. O. Schweitzer, III, A. Guzmán, M. V. Mynam, V. Skendzic, B. Kasztenny, and S. Marx, "Locating Faults by the Traveling Waves They Launch," proceedings of the 67th Annual Conference for Protective Relay Engineers, College Station, TX, March 2014.

[3] SEL-T400L Time-Domain Line Protection Instruction Manual. Available: selinc.com.

[4] A. Guzmán, G. Smelich, Z. Sheffield, and D. Taylor, "Testing Traveling-Wave Line Protection and Fault Locators," proceedings of the 14th International Conference on Developments in Power System Protection, Belfast, United Kingdom, March 2018.

[5] L. V. Bewley, Traveling Waves on Transmission Systems. Dover Publications, New York, NY, 1963.

[6] E. O. Schweitzer, III, A. Guzmán, M. Mynam, V. Skendzic, B. Kasztenny, C. Gallacher, and S. Marx, "Accurate Single-End Fault Location and Line-Length Estimation Using Traveling Waves," proceedings of the 13th International Conference on Developments in Power System Protection, Edinburgh, United Kingdom, March 2016.

VIII. BIOGRAPHIES

Stephen Marx received his BSEE from the University of Utah in 1988. He joined Bonneville Power Administration (BPA) in 1988. He is presently the District Engineer in Idaho Falls, Idaho, for BPA. He has over 30 years of experience in power system protection and metering. He has been a lecturer at the Hands-On Relay School in Pullman, Washington, since 2007. He is a registered professional engineer in the state of Oregon. He is a member of IEEE and has authored and coauthored several technical papers.

Yajian Tong holds a master's degree in electrical and computer engineering. He is currently a research engineer with Schweitzer Engineering Laboratories, Inc. He is a member of IEEE.

Mangapathirao V. Mynam received his MSEE from the University of Idaho in 2003 and his BE in electrical and electronics engineering from Andhra University College of Engineering, India, in 2000. He joined Schweitzer Engineering Laboratories, Inc. (SEL) in 2003 as an associate protection engineer in the engineering services division. He is presently working as a principal research engineer in SEL research and development. He was selected to participate in the U.S. National Academy of Engineering (NAE) 15th Annual U.S. Frontiers of Engineering Symposium. He is a senior member of IEEE and holds patents in the areas of power system protection, control, and fault location.